A methodology for assessing the impact of salinity gradient power generation in urban contexts

A. Cipollina, M. L. Di Silvestre, F. Giacalone, G. M. Micale, E. Riva Sanseverino, R. Sangiorgio, Q. T.T Tran, V. Vaccaro, G. Zizzo

Affiliation: Università di Palermo, Italy

Abstract **—** The paper proposes a methodology to assess the potential impact of salinity gradient power technology in urban contexts. The idea to employ such energy source in urban contexts derives from the observation that, among the energy districts outputs, low-salinity treated wastewater can be used to produce electricity if a suitable source of high salinity feed (seawater of a salt-works) is also available.

The methodology uses the HOMER software for assessing the district's electric energy production, consumption and exchange with the main grid. Then, starting from the total gross surface and the number of inhabitants of the district, some possible realistic scenarios characterized by different wastewater flow rate are defined. Finally, for each scenario the size and the yearly energy production of the salinity gradient power system are calculated thanks to a simulator carried out by the same authors.

An application example, considering three different scenarios, shows that urban density plays a crucial role in the process and that the most promising realistic scenarios are those including treated wastewater and brine and unlimited seawater and brine.

The economic feasibility of the salinity gradient power technology is evaluated by a comparison with classical renewable technologies such as photovoltaic and wind systems.

Keywords **—** ***Salinity gradient power; Urban energy hub; Sustainable cities; HOMER.***

1. Introduction

The increased widespread use of electrical equipment, resulting in a growing electricity demand, and the highly constraining environmental objectives push for the integration of renewable energy sources (RES)s in power systems [1]-[3]. Although fossil sources still play a key role in energy supply, they are strongly polluting and on the road to get exhausted. The research about new energy sources to strengthen power supply is thus necessary. These sources not only contribute to improve life quality and meet consumer

demand for electricity, but they also need to meet environmental criteria. Cities in particular, accounting for 70% of CO_2 emissions worldwide, are called for identifying clean energy sources that can be well integrated into the urban environment [4]. On the other hand, the huge electrification will impose on electricity production a further sustainability challenge. In the last years, more than 6000 European cities have signed up to the Covenant of Mayors. The latter is a bottom-up initiative consisting in a voluntary commitment to achieve, on average and at city level, a 28% cut in CO_2 emissions by 2020, i.e. 8% more than the EU's 2020 target. Most of the papers that can be found in the literature about providing renewable electricity in urban contexts report about off-site installations or rural applications. A recent paper [5] shows the feasibility of hybrid generation in cities and rural areas, comparing different alternatives for supplying a small electrical load for telecommunications, a Base Transceiver. The order of magnitude is of some kWs. The study compares different alternatives for producing electricity such as: PV-Diesel-Battery, PV-Wind-Diesel, Wind-Diesel-Battery, Wind-Diesel, PV-Diesel system. The architectures are studied considering four urban sites in India in the region of Punjab. In this paper, no mention is made about the possibility to implement these solutions in urbanized areas, considering acoustic, visual impact or even safety of the considered solutions. Other papers report about the conventional renewable-based solution adopted for cities lighting in China [6]. Street lamps in most Chinese urban environments are supplied by wind–solar hybrid electric generation systems. Some papers concentrate on building PV integrated solutions such as [7]. The paper proposes a techno-economic analysis of the installation of roof-top and vertical facades, including windows, PV generators for two large buildings in the Kingdom of Bahrain. The amount of electricity extracted for one of the two building is 3 million kWh in 1 year, enough to supply electricity for 171 houses in the region. The solution provides an annual CO_2 reduction of 3000 Ton with the considered energy mix of Kingdom of Bahrain. However, the reported examples refer to areas where such solutions are easier to integrate, as compared to European areas where historicized urban environment provide a further challenge. [8] shows that off-site installations have a smaller payback period as compared to on-site installations of solar photovoltaic electricity generation, although both show competitive LCOE. The study assessed the technical feasibility and economic viability of a 2.5 MW photovoltaic power plant for supplying a garment zone in Jaipur, India, considering on-site and off-site options. The work in [9] proposes an economic feasibility of using solar PV in urban contexts in China, in the city of Xi'an. The sizing of the storage is strongly related with the load profile features. The latter are quite different when considering commercial or residential buildings. The matching between the load and the solar radiation profile affect the Cost of Energy of the system. Another important issue affecting the Cost of Energy is certainly the S/V ratio. The study in [9] analyzes a commercial office block (10000 m^2) and an independent villa. The study does not

account for multi-level buildings for which the electricity demand density is quite higher. An interesting study from K. Steemers connects urban form and energy consumption [10]. What appears is that the use of buildings and the urban density are two main issues for defining energy consumption. As a result, the electric load profile, that is so important to determine the cost of energy of renewable sources in cities, may change as an effect of energy efficiency of electric appliances which has improved dramatically in recent years and the demand response and aggregation of electrical loads carried out for market purposes or for technical reasons. Other papers focus on the role of Zero Energy Buildings [11]-[13], namely buildings where energy consumption is reduced and Energy Management Systems control loads and distributed energy resources. Out of the latter, the generation resources use renewable sources.

What appears from this overview there are not so many solution for urbanized environments, especially where highly historicized contexts are present. Moreover, renewable energy production solutions in cities must be safe and low impact. In this paper, Salinity Gradient technologies are introduced as a state of art clean electrical energy source. Salinity Gradient Energy (SGE) or Salinity Gradient Power (SGP) is a novel source of energy available whenever two solutions with different salinity levels are mixed together, as occurs in nature when a river discharges into the sea. The harnessing of this energy requires a suitable device able to perform a 'controlled mixing' of the two streams at different salinity (e.g. river water and seawater). Such operation thus results in the recovery of the mixing energy available rather than in its complete dissipation. Sustainability of SGP is ensured by the hydrological cycle, which guarantees the reestablishment of the original streams and salinity levels. For this reason, SGP is a very clean form of renewable energy that does not produce any CO_2 emission and presents very low environmental footprint. Furthermore, it is suitable for continuous power production as it is not affected by the typical discontinuities of other renewable energy sources (e.g. solar, wind, tidal, etc.), at the contrary, being a possible "chemical energy flywheel" for RE-powered systems requiring energy buffering strategies [15].

The present work explores the possibility to include SGP into a urban energy hub, namely an energy district. An energy hub is a system where different kinds of energy carriers are converted, stored and distributed in order to satisfy energy demand [14]. An optimized consumption of the different sources guarantees efficiency of the hub as a whole, by analytically expressing the relationship between input and output energy carrier flows [15]. RESs are used popularly in energy hubs like solar, wind, biomass, biogas, sea water, waste water, etc. Using suitable technologies for conversion and management can reduce at its maximum the use of storage, by replacing one energy source with another when renewable energy is missing or when it is not sufficient. The energy hub model and its optimized management can make sure that the potential of renewable energy will be exploited to its maximum. Besides, in the energy hub, the combination between

heat and power systems is the most beneficial technology in order to generate heat and electricity and to reduce operating costs, enhance system optimization, improve energy use efficiency, while satisfying environmental targets. In this work, we analyze the benefit that the SGP technology can bring to the energy hub model with a specific focus on urbanized contexts. Recently, many studies investigated the integration of renewable energy systems in urban areas [16]-[21]. It was showed that an effective option to increase local renewable energy production is to convert surplus electricity into other kinds of energy like thermal energy [22]-[24] and the work is implemented with different modelling approaches and simulation tools [25]. However, these research works only analyze the integration of solar [26], [27], wind [28]-[30] and biomass [31] sources. To the authors' knowledge, the integration of SGP production within an urban energy hub has not been analyzed yet and is therefore an interesting option to be fully explored.

For this reason, in this paper an analysis methodology to assess the potential impact of salinity gradient power technology in urban contexts and an application to a case study are presented.

In this research, the HOMER PRO software supports the analysis of the potential impacts of SGP on the electric energy consumption of an urban district. Different scenarios with various population densities have been investigated for a small urban center. The difference in population density indeed leads to different amounts of wastewater production. Assuming that wastewater is treated using an advanced Membrane BioReactor, MBR [32], the treated effluent will constitute a suitable low-salinity stream for feeding the SGP system. The results demonstrate that in certain conditions the adoption of such technology could relieve the system from dependency from the grid, although other scenarios with increased population densities need to be investigated for a full understanding of the idea.

The remainder of the paper is organized as it follows:

- Section 2 contains a brief presentation of salinity gradient power technologies and of the previous work on the authors on this subject;
- Section 3 describes the methodology used for sizing a SGP generator for an urban district and for evaluating its impact on the energy balance of the whole urban center;
- Section 4 reports a feasibility study based on the methodology presented in Section 3;
- Section 5 contains a discussion on the results of the study and on the economic feasibility of SGP systems;
- Section 6 contains the conclusion of the paper.

2. **Salinity gradient power technology**

In 1954, R. E. Pattle drew up a study called "Production of Electric Power by mixing Fresh and Salt Water in the Hydroelectric Pile" [33]. The study presented for the first time the potential of an untapped source of energy manifesting itself when a river flew into the sea. This form of energy was created from the osmotic pressure difference between the water of the river and the sea water. In 1973, Sidney Loeb, a professor at Israel Ben-Gurion University, presented a method for generating energy by means of the so called Pressure Retarded Osmosis concept (PRO). In 1977, the same author presented a second process, which generated electricity through a Reverse Electro-Dialysis (RED) process. Both methodologies do not cause any emission of carbon dioxide (CO_2) or any costs for fuel as reported by Jones and Finley studies in the article "Recent Development in Salinity Gradient Power" [34]. Their studies demonstrated that the higher the difference of concentration between the two effluents, the greater the potential energy obtained from the SGP technology.

2.1. Pressure Retarded Osmosis (PRO) technology

In a PRO system, two different salinity solutions are separated by a semi-permeable membrane. The membrane lets the solvent (i.e. water) to permeate while it rejects the solute (i.e. dissolved salts). The difference of chemical potential (more often seen as difference in osmotic pressure) between the two solutions causes the transport of water from the dilute solution to the concentrate one. If pressure is applied to the concentrated solution, the transport of water is partially retarded and thus the transport of the latter from the low-pressure dilute to the high pressure concentrate solution implies a pressurization of the transported volume of water, which can eventually be used to generate power in an external turbine. The indisputable advantage of this process is that the sources are virtually unlimited. Another advantage is the production of a "waste" stream simply constituted by brackish water, easily disposable or reusable by further industrial applications. However, the Technology Readiness Level (TRL) is still strongly influenced by the lack of suitable membranes able to operate at optimal conditions in a wide range of operations.

2.2. Reverse Electro-Dialysis (RED) technology

In a RED system, a number of anionic and cationic membranes are stacked in alternating manner between an anode and a cathode as shown in Figure 1.
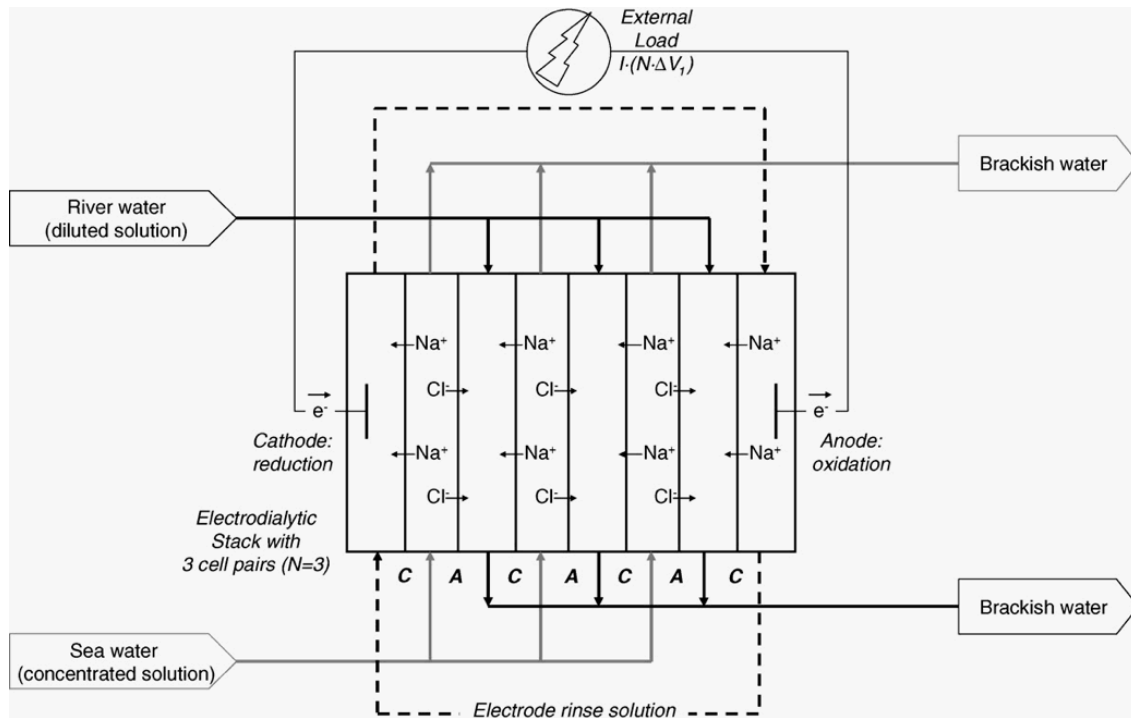
Fig. 1. Functional diagram of the RED technology.

The compartments created by the membranes are filled in an alternating manner with a concentrate and a dilute solution, respectively. The salinity gradient generates a potential raise at each solution/membrane interface (namely, the cell pair potential or the electromotive force of the pile, being around 80 mV per membrane pair when combining sea water and river water). The difference of chemical potential also causes the transport of ions through the membranes from the concentrate towards the dilute solution, which are forced to migrate in a controlled way (cations will move through the cation exchange membrane and anions through the anion exchange membrane, respectively), thus generating an ionic current through the membranes stack. At the end of the stack, two electronic compartments allow to convert the ionic current into an electronic one. As a result, an electron can travel and then be transferred from the anode to the cathode through an external electrical circuit. Thus, the electrical current and the potential difference generated at the electrodes can finally be used to generate electrical power when an external load or an energy consumer is connected to the circuit.

The RED process can be operated continuously by means of a constant supply of two streams with different salinity. Until now, research has focused on the combination of water at low salt concentration and seawater. However, this approach has serious limitations due to the low salinity solution, which significantly increases the electrical resistance of the stack. Within the EU-funded REAPower project (www.reapower.eu), researchers found the way to overcome this limitation by using brine and saline water for the production of

electrical energy. Laboratory investigations [35]-[37] and modeling activities [38],[39] have identified a number of crucially important parameters, which helps in design, and optimize RED units. In particular, RED units operating with artificial solutions at laboratory scale have been demonstrated to reach power generation density higher than 4 W per each square meter of membrane cell pair area [40], when operating with seawater-like concentrations. When passing to desalination brines and to ultra-concentrated brines (such as those availabile in saltwroks) power density could reach values above 10 W per square meter of cell pair area [41],[42], thus boosting the potential for economical competitiveness of this technology. An important milestone of such recent developments has been the installation of a RED pilot plant in Marsala saltworks (Trapani, Italy) operating with concentrated brines and saline solutions [43],[44]. The prototype is the first plant operating in such conditions and has reached the largest power production ever registered so far worldwide. The REAPower project proved that with the configuration employing seawater and brine the energy density can reach values above 1 MJ/m^3 giving rise to a power production of almost 1 kW for the plant operating in a real environment.

ELECTRIC POWER 4.3 kW

BRINE
SALT CONCENTRATION:
4 mol/l
FLOW RATE:
310 m³/day

STACK SGP

- 5.6 MJ/m³$_{brine}$ (theoretical)
- 1.2 MJ/m³$_{brine}$ (practical)
- Size 2.25 m³
- 1500 m² of membrane

TREATED WASTEWATER (TWW)
SALT CONCENTRATION:
0.01 mol/l
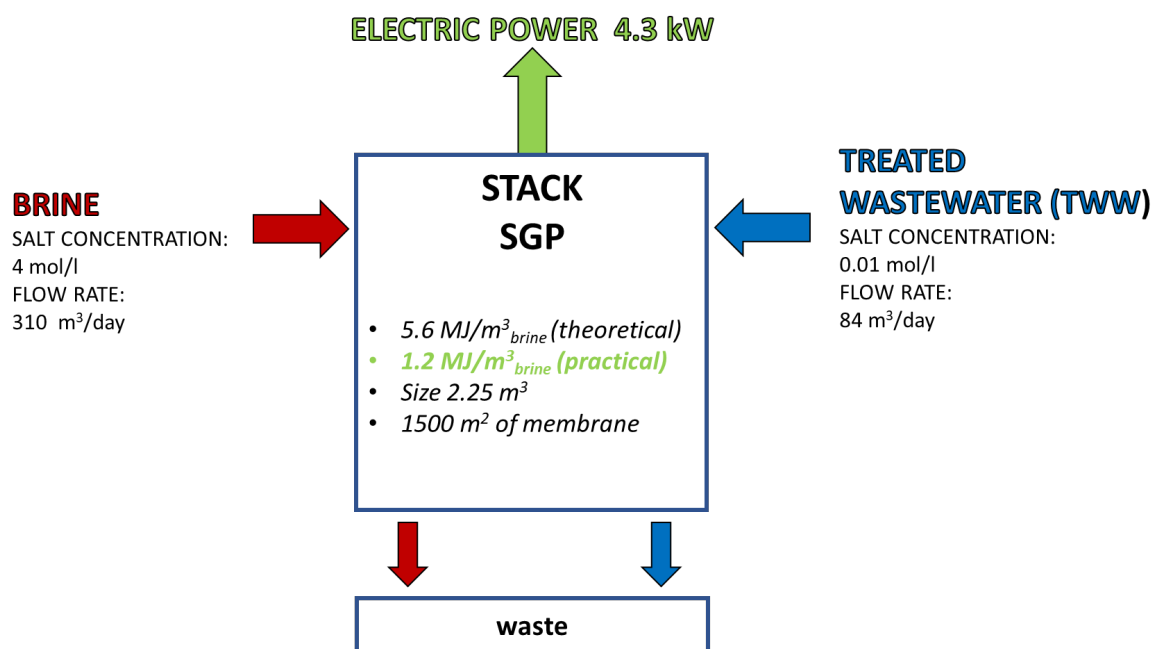FLOW RATE:
84 m³/day

waste

Fig. 3. Schematics of the mass and energy input/output in a RED unit, as analyzed in the present work (scenario 1.A).

This technology has a great potential: the electricity is produced simply from water supplies with different concentrations of salt and is clean, quiet, and does not include moving parts. The only waste product is brackish water. In this paper, the case studies will be implemented based on the application of this promising energy production technology.

3. Methodology

In this section, a methodology is proposed to assess the impact of SGP technology in urban contexts in terms of coverage of the energy consumption in a period of one year. The methodology adopts two different simulation tools (Figure 3):

- the Hybrid Optimization Model for Electric Renewables (HOMER) PRO v. 3.7.3.0 software, a product of the National Renewable Energy Laboratory (NREL);
- a simulation tool of the RED process (in the following RED simulator) implemented at the University of Palermo within the REAPOWER project.

By HOMER, the energy hub can be easily modelled and different scenarios can be assessed based on technical and economic aspects. On the other side, the RED simulator implements a lumped parameter RED model, previously developed by the same authors **Errore. L'origine riferimento non è stata trovata.**, [46], able to evaluate the RED energy production for a given scenario.
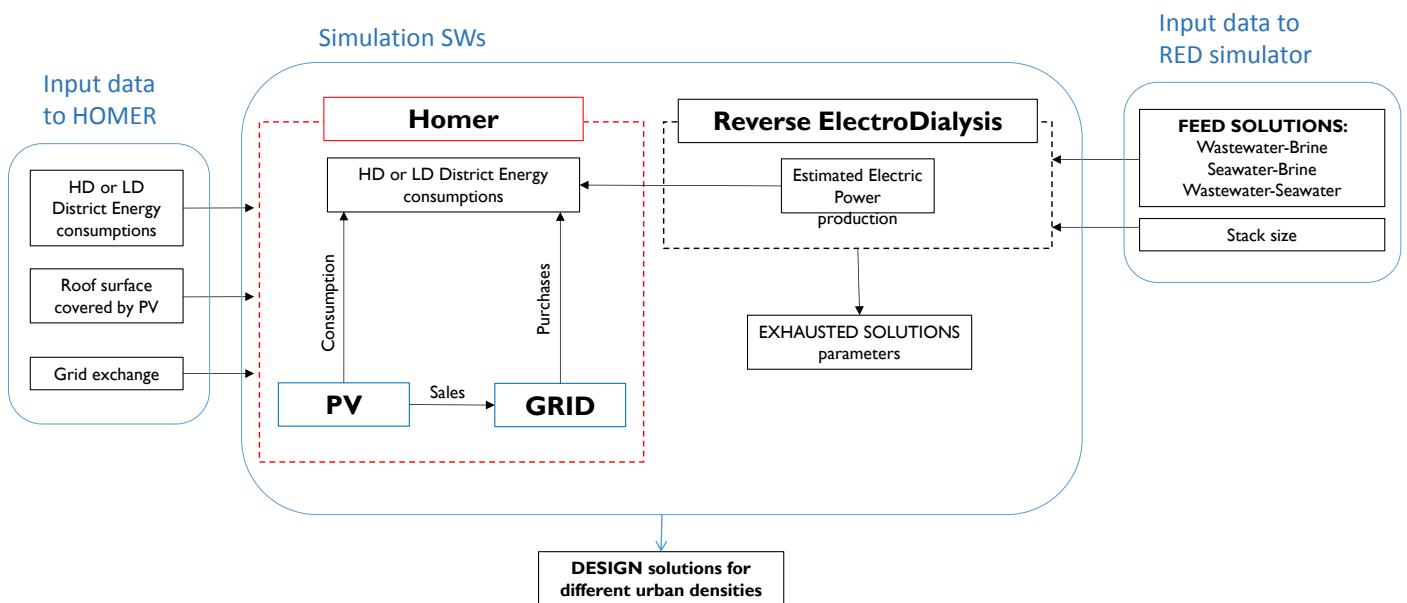

Fig. 3. Combination of the simulation tools.

The methodology, whose flow chart is represented in Figure 4, is made by the following steps:

- the boundaries of the urban district are individuated;
- the energy consumption of the district, the energy production from distributed generation and the energy exchange with the main power system supplying the microgrid serving the urban district, are

evaluated (calculated with simulations or measured) considering one year and sent to HOMER as input data;

- possible realistic scenarios characterized by different wastewater flow rate and effluents concentration are defined starting from the total gross surface and the number of inhabitants of the district. The effluents' data are sent to the RED that sizes the SGP system and calculates the yearly energy produced by the RED process. The yearly production of the SGP system is sent to HOMER;

- HOMER evaluates the percentages of coverage of the energy district's consumptions from the grid, from the PV systems and from the SGP system.

The proposed methodology is very easy to implement since it adopts simple energy calculations starting from the mathematical models of the various loads and generation technologies.
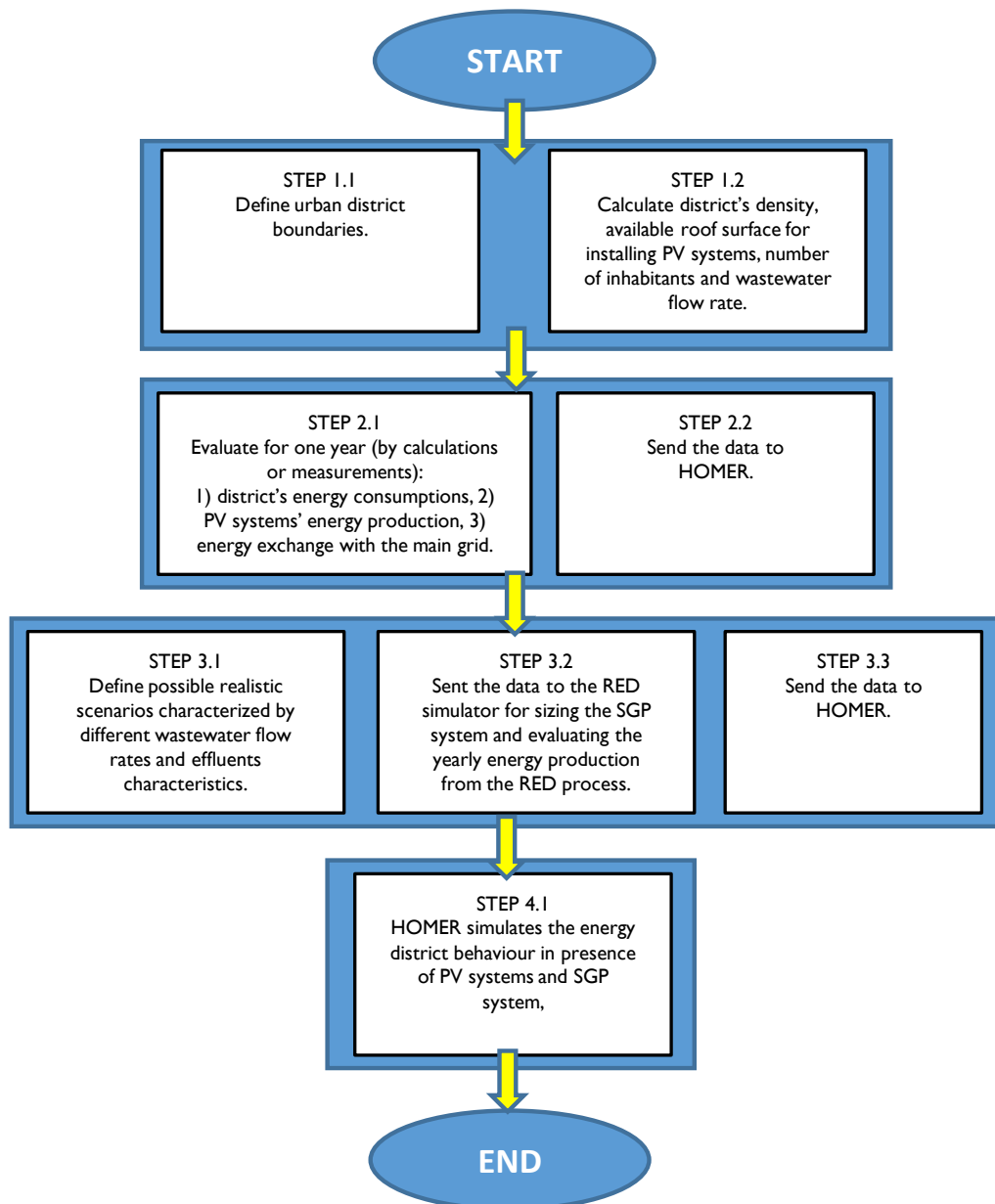
Fig. 4. Flow chart of the proposed methodology.

3.1. RED simulator

The RED simulator is based on a deterministic model of the SGP system, in which all the main phenomena involved in the process are described. The model is implemented on Excel spreadsheets and adopts purposely-developed macros (Figure 6).

According to the adopted lumped parameter approach, properties and variables involved in the calculation are evaluated at the average (inlet-outlet) concentration of the two streams (dilute and concentrate). The flow chart reported in Figure 5 duly illustrate the calculation algorithm adopted. The solving routine starts

calculating average concentrations of the two solutions from inlet concentrations and assuming the outlet concentrations ($C^k_{out,dil}$ & $C^k_{out,conc}$). After fixing the inlet dilute and concentrate flow rates, membrane properties (permselectivity, resistances and salt permeability) and RED stack size, the model estimates the main fluxes and electrical variables involved in the process. Finally, outlet solutions concentrations ($C^{calc}_{out,dil}$ & $C^{calc}_{out,conc}$) are evaluated from mass balance equations. If the calculated outlet concentrations are different from the two assumed in the first step, a new iteration is performed startin from the new values of outlet concentrations and the procedure is repeated until convergence is obtained ($C^{calc}_{out,dil}= C^k_{out,dil}$ & $C^{calc}_{out,conc}= C^k_{out,conc}$).

A brief description of the model equations is reported below, while a more detailed description along with the model validation with experimental results are reported in [45],[46],[38].
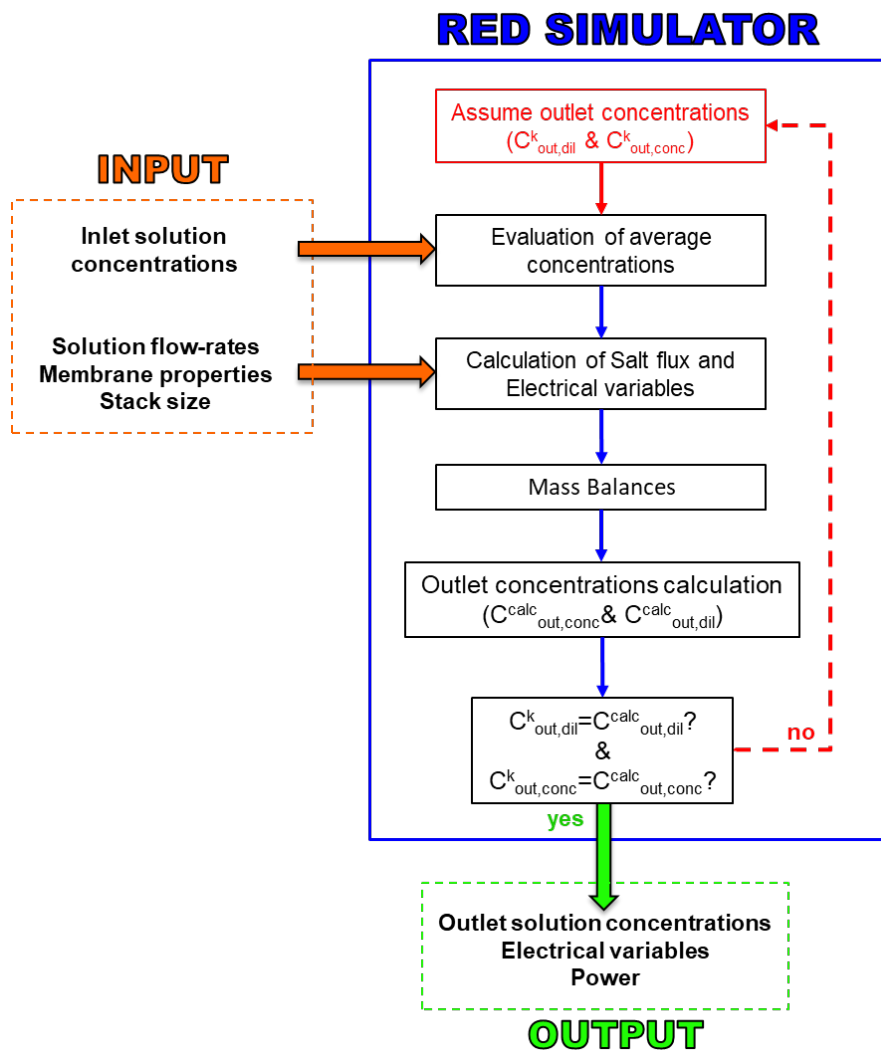

Fig. 5. Flow chart of the RED simulator.

Fixing the flow rate (F_{conc} or F_{dil}) and a velocity (v_{dil} or v_{conc}) of the stream with limited availability in the unit, the number of cell pair is calculated according to the following equations:

$$F_{conc} = N v_{conc} \delta_m b \varepsilon \qquad (1)$$

Where N is the cell pair number, b is the width of the stack (b= 1 m) and ε the porosity of the channel due to the spacer presence (0.825).

The electro motive force (emf) produced across the couple of Ionic Exchange Membranes (IEMs) is determined according to the Nernst's equation, using the average concentration of dilute and concentrate solutions within the two channels:

$$E_{cell} = N * (\alpha_{AEM} + \alpha_{CEM}) \frac{RT}{F} \ln \left(\frac{\gamma_{conc,av} m_{conc,av}}{\gamma_{dil,av} m_{dil,av}} \right) \qquad (2)$$

Where α_{CEM} and α_{AEM} are the average permselectivity of cationic and anionic exchange membrane, respectively, $\gamma_{conc,av}$, γ_{dil}, $m_{conc,av}$ and $m_{dil,av}$ are the average activity coefficients and average molarities of the two solutions feed in the system, R is the ideal gas constant, T is temperature and F is Faraday's constant.

However, when current circulates through the stack, the electrical potential of the RED stack at the external electrodes is given by:

$$E_{stack} = E_{cell} - R_{stack} I \qquad (3)$$

R_{stack} is the stack resistance, defined as the sum of the resistances constituting the cell pairs pile and the resistance of electrodic compartments (R_{blank}):

$$R_{stack} = N R_{cell} + R_{blank} \qquad (4)$$

with

$$R_{cell} = R_{dil} + R_{conc} + R_{AEM} + R_{CEM} \qquad (5)$$

Where R_{cell} (single cell pair resistance) is obtained by summing membranes (R_{CEM} and R_{AEM}) and channels (R_{dil} and R_{conc}) resistances.

The electrical current circulating in the system for a given external load is equal to:

$$I = \frac{E_{stack}}{R_{ext}} \tag{6}$$

where R_{ext} is the electrical resistance of the external load connected to the pile.

It is worth mentioning that the achievable power density can be maximized when this external resistance is equal to the internal one (i.e. R_{stack}) as often happens in power generators with internal resistance dissipations.

Finally, the power output from the unit can be calculated as:

$$P = E_{stack} * I \tag{7}$$

In addition to the above presented equations for electrical variables, the model predicts the salt flux across each membrane by accounting for the two different transport mechanisms: (i) the columbic flux related to the counter-ions migrating due to the electrical current and (ii) the diffusive salt flux due to the diffusion of neutral salt through the membranes (non-ideal phenomenon, which depletes the salinity gradient without generating electricity). Mathematically, this can be described as:

$$J_{salt} = \frac{I}{AF} + 2 \frac{D_{salt} (C_{Conc,av} - C_{dil,av})}{\delta_m} \tag{8}$$

Where I/A is the current density with respect to the cell pair area and is divided by the Faraday constant in order to give a molar flux, δ_m is the IEM thickness (equal to $1.25E^{-4}$ m) and D_{salt} is the salt diffusive permeability, formally analogous to a salt diffusion coefficient, which could be directly derived from membrane permselectivity

Finally, outlet concentrations are calculated solving mass balances for dilute and concentrate channels:

$$C_{low,out} - C_{low,in} = \frac{J_{salt} A}{Q_{low}} \tag{9}$$

$$C_{conc,out} - C_{conc,in} = - \frac{J_{salt} A}{Q_{conc}} \tag{10}$$

The model does not need the solution of complex optimization problems for evaluating the size of the system and its potential electricity production. The only data needed for the RED simulator are the effluents' characteristics and the wastewater flow rate, on the basis of the district's density. For this reason, the

proposed methodology can be adopted easily for practical application, such as feasibility studies or preliminary design of SGP systems.
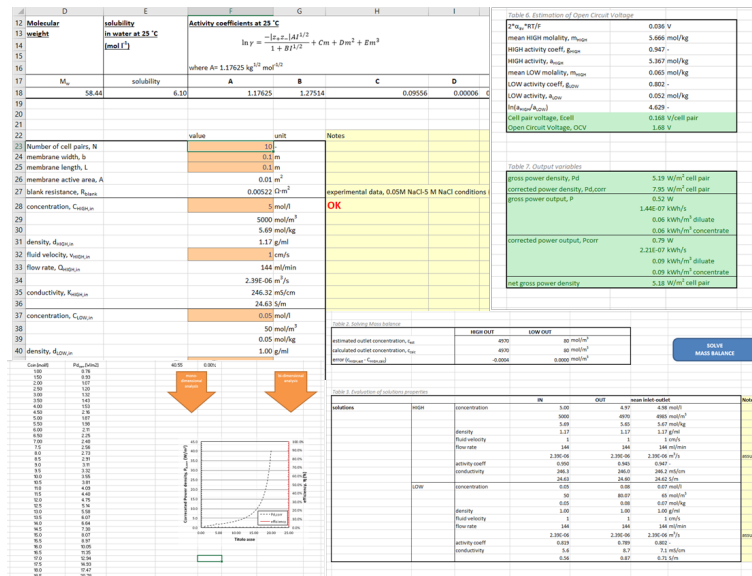

Fig. 6. Screenshot of the main sheet of the RED simulator.

4. Results

4.1. Feasibility study for the design of a SGP system: energy consumption and production

The feasibility study for the installation of a SGP system is carried out for an urban center characterized by the presence of two areas where it is possible to identify two different districts (Figure 7):

- a Low density (LD) District: residential area including large part of terraced houses or newly built isolated houses, composed of 22 buildings hosting as many households;
- a High density (HD) District: residential area composed of 55 buildings hosting 140 families.

In order to perform the energetic analysis for a realistic situation, the urban center has been chosen with the characteristics of the town of Mussomeli (geographic coordinates: 37°34'32"N, 13°45'11"E) in the South of Italy, from which the energy consumptions are available from a previous study [48].
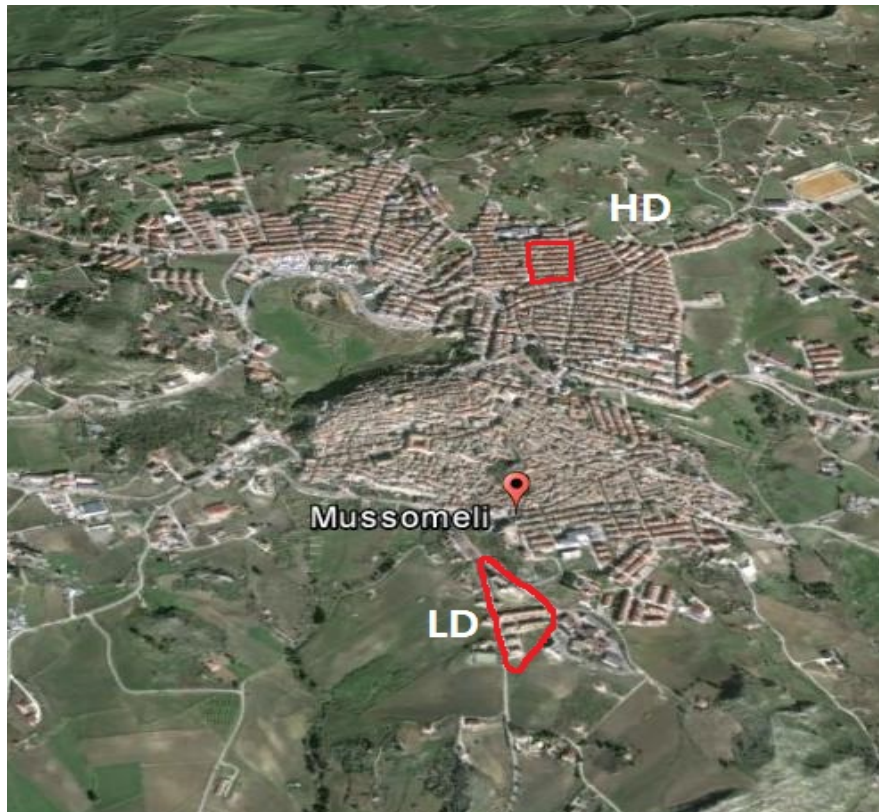
Fig. 7. The position of LD district and HD district in Mussomeli.

The yearly electricity consumptions of the two districts are obtained assuming that every house contains the same appliances whose yearly electric consumptions are reported in Table 1. For simplicity, an uniform monthly representation of these consumptions is assumed. The only variability is related to the adoption of electric air-conditioning systems during summer, as shown in Figure 8. The figure clearly shows the electric consumptions of the appliances and of the cooling system for every months for both the LD and the HD districts. In both cases, electric consumptions are assumed lower from November to April and higher from May to October.

Table 1. Electric appliances consumptions

	Diffusion		LD district		HD district	
	%	Load's consumption (kWh/year)	Houses	District's consumption (kWh/year)	Houses	District's consumption (kWh/year)
Fridge without freezer	30	321	7	2247	42	13482
Fridge with freezer	70	572	15	8580	99	56628
Freezer	30	464	7	3248	42	19488
Washing machine	97.3	358	21	7518	137	49046
Dishwasher	14.6	361	3	1083	21	7581
Lighting system	100	434	22	9548	141	61194

TV	136.6	219	30	6570	193	42267
Hi-Fi	46.8	95	10	950	66	6270
Computer	31.9	91	7	637	45	4095
Electric iron	90	150	20	3000	127	19050
Electric oven	50	100	11	550	71	7100
Microwave oven	20	110	4	440	28	3080
Others	100	80	22	1760	125	11280
Total				**46131**		**300561**

A rooftop photovoltaic (PV) generation system is supposed installed in every building of the two districts, with PV panels mounted on the south-oriented surface of the roof. The area available for their installations is reduced with respect to the total roof surface, considering the presence of shadows due to difference in height of buildings, by means of the software Sketchup (Google). The overall installed PV power is finally calculated assuming to use PV modules with rated power 327 W and size 1559x1045 mm. Figures 9 and 10 show the 3D rendering of the districts with PV panels.
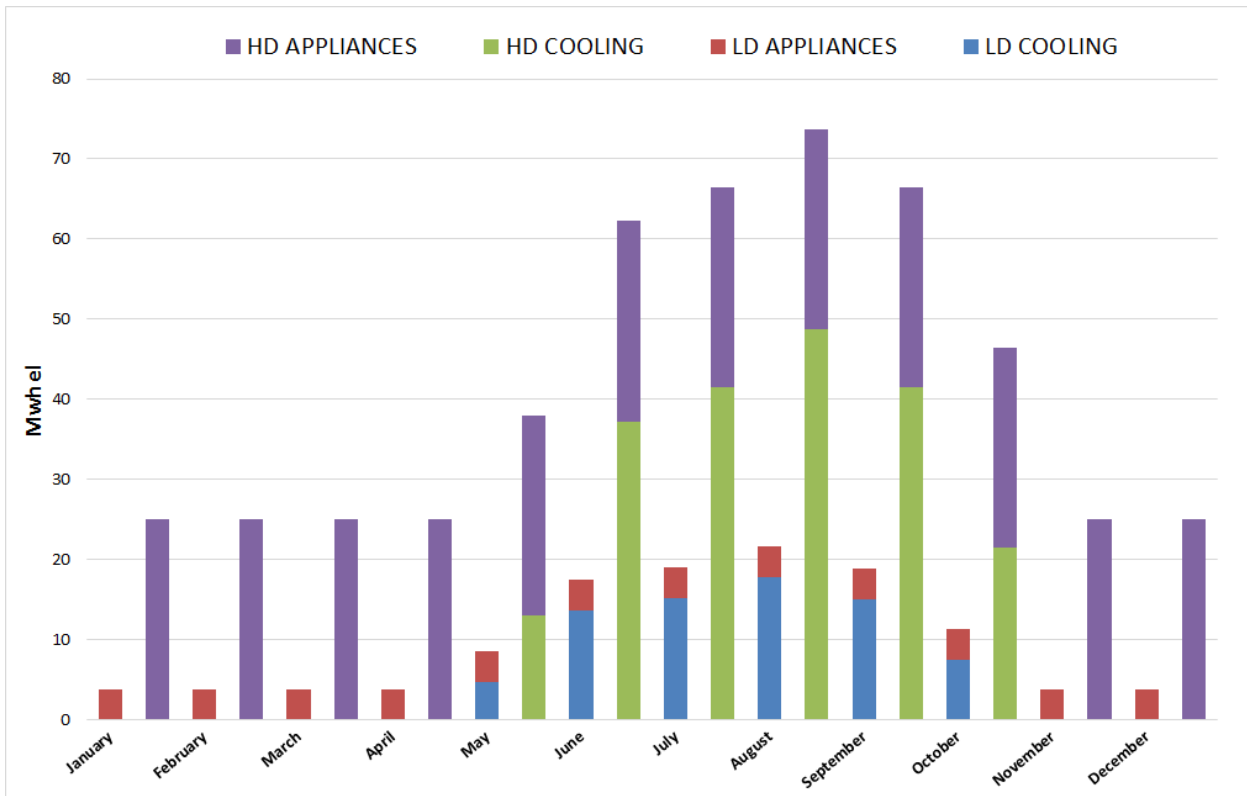

Fig. 8. Total electricity consumption per month..

Fig. 9. 3D rendering of LD district with PV panels.

Fig. 10. 3D rendering of the HD district with PV panels.

As shown in Figure 11, in this condition PV generation does not support fully the electricity consumptions of the districts, thus further measures are needed to cover the loads' needs.
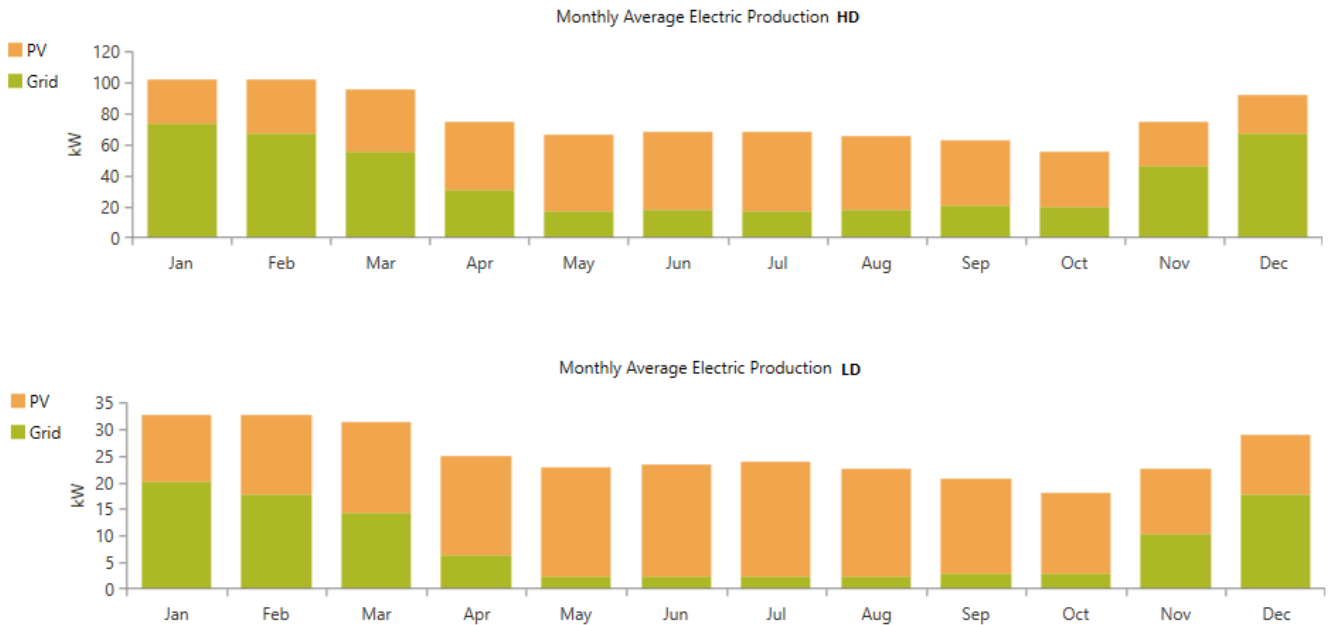
Fig. 11. Monthly power supply for the two districts considering PV generation, using HOMER.

HOMER also considers the possibility to sell electricity to the grid, since the system here considered does not implement any storage unit, the non-perfect superposition of consumption and PV generation produces the situation depicted in Table 2. Figure 12 shows the mask of a screenshot of HOMER where the district's electric loads, the PV plants and the grid are schematically represented as connected to the same bus.
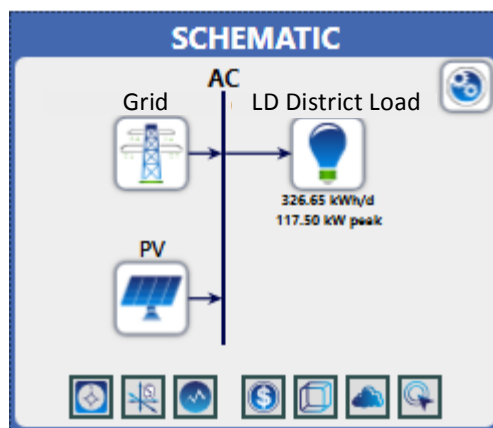

Fig. 12. Schematic representation of the considered architecture using HOMER (LD district).

In Table 2, the PV production is 147613 kWh/year in the LD district and 346918 kWh/year in the HD district. The energy purchased from the grid is 74222 kWh/year in the LD district and 327704 kWh/year in the HD district, respectively. In the LD district, the percentage of coverage of energy consumption with PV generation without considering the excess energy sold to the grid, is equal to 37.75%. In the HD district, the coverage is instead 34.96%. When considering the overall load coverage the percentages refer to 119229 kWh/year in the LD district and to 503886 kWh/year in the HD district.

In the following, some scenarios are considered with the aim of covering a percentage of the energy purchased from the grid (*Grid Purchases*) using the RED technology. The scenarios will also account for the coverage of the overall load.

Table 2. Output of HOMER simulation.

LD District			HD District		
Production	**kWh/year**	**%**	**Production**	**kWh/year**	**%**
PV system	147613	66.54	PV system production	346918	51.42
Grid purchases	74222	33.46	Grid purchases	327704	48.58
Total	221834	100.00	Total	674622	100.00
Consumption	**kWh/year**	**%**	**Consumption**	**kWh/year**	**%**
Loads	119229	53.75	Loads	503886	74.69
Grid sales	102606	46.25	Grid sales	170736	25.31
Total	221834	100.00	Total	674622	100.00

4.2. Scenarios

Two different scenarios are defined:

1) urban center close to a salt-works;

2) urban center close to the sea.

For the first scenario the following sub-cases are considered:

1.A) limited wastewater flow rate;

1.B) unlimited seawater flow rate.

For the second the following sub-case has been considered:

2) limited wastewater flow rate.

As already specified, the SGP production is based on the use of two effluents: a diluted or low concentration (LC) effluent and a high concentration (HC) effluent. Therefore, the following possible combinations of effluents are considered:

- treated wastewater (LC) and brine (HC);

- seawater (LC) and brine (HC);

- wastewater (LC) and seawater (HC).

Table 3 summarizes the situations considered.

Table 3. Definition of the considered scenarios.

Scenario	LC	HC
1.A	Treated wastewater (limited flow rate)	Brine
1.B	Seawater	Brine
2	Treated wastewater (limited flow rate)	Seawater

In the cases 1.A and 2 wastewater is considered as LC solution in the RED stack. The corresponding cell pair number is determined selecting a reasonable solutions velocity (0.2-1.0 cm/s) in the RED channels. The brine flow rate is fixed at a value ranging from 300 m^3/d to 350 m^3/d, typically available quantity in aside located close to a small-medium size salt-works.

4.3. Wastewater production estimation

Residential wastewater comes from residential buildings and services deriving from the urban metabolism and domestic activities. The sizing of the wastewater treatment plant must be done based on the number of equivalent inhabitants (AE). According to the Italian legislation [47], one AE can be defined differently according to the parameters that are considered:

- biochemical demand of oxygen in 5 days (BOD_5) equal to 60 g/day;
- chemical demand of oxygen (COD) of 130 g/day or corresponding to a discharge volume of 0.2 m^3/day for inhabitant, considering the highest value.

The reference legislative decree 152/06 [47] establishes that one AE occupies 35 m^2, or fraction, of gross surface in residential buildings, for which a volume of wastewater equal to 0.2 m^3 can be considered. In the considered case, up to 0.2 m^3/AE are considered for the HD district and 0.25 m^3/AE for the LD district considering slightly higher production for gardening and other activities. The gross surface of the houses varies in the two considered cases (LD and HD). What is done here is that the overall built surface is considered and then it is divided by the number of families so as to find the overall surface that can be ascribed to each home as shown in Table 4.

Table 4. Calculation of wastewater production from the number of AE.

	LD District built surface [m^2]	HD District built surface [m^2]
Total surface	2081 (22 buildings)	11983 (55 buildings)
Families	22	141
Single surface of one flat/house	94.59	84.98

It turned out that each family has 3 AE both for the LD and the HD district.

In order to get the number of liters of wastewater produced, it will be necessary to multiply the number of houses by the number of AE and by the number of liters produced as fixed by the norm. It will turn out that the houses in the LD district produce 16.5 m³/day and the HD district produces 84.6 m³/day. This water is pumped into the MBR system [27] that substitutes the activated sludge technology for depuration. This depuration technology is more efficient and the depurated water shows a high degree of chemical, physical and bacteriological purity. By these special membranes, it is decided to proceed to the depuration of the wastewater produced by the users in the two districts in order to attain depurated water for the electricity production through RED technology.

4.4. Use of the simulator for detecting the energy production from SGP in different scenarios

The developed RED simulator allows to simulate the behavior of a real stack with its size and specific operating conditions, thus providing a useful tool for assessing the feasibility of the SGP project in urban environment. The single stacks considered in the simulations have the following features considering the different urban densities and thus the amount of available wastewater:

- number of cell pairs N = 300 ÷ 1000;
- membrane size S = 1 m²;
- membrane thickness δm = 0.125 mm.

However, when larger membrane area is required, multiple stack assembly can be considered, by connecting in parallel a number of stacks with 1000 cell pairs.

In the following the results of the calculations for the two scenarios are reported.

Scenario 1

In Scenario 1, the salt concentration for the wastewater flow rate depurated using the MBR technology [32] can be assumed as $C_{LC, IN}$ = 0.01 mol/l, while the brine shows a concentration of $C_{HC,IN}$ = 4 mol/l. In both cases 1.A and 1.B, since the district is close to a salt-works, the quantity of brine can be assumed as unlimited, while the same can not be said for wastewater. Velocities of effluents in all cases are chosen small to limit the need of electricity for the pumping system. Scenario 1.A is thus more realistic than scenario 1.B.

In Scenario 1.A, the flow rate of wastewater has been calculated in 84.6 m^3/day for the HD district and 16.5 m^3/day for the LD district. The choice of the number of cell pairs in all the cases presented below is done considering the experiments carried out in the REApower project and the experience of the authors. Table 5 summarizes the data for scenarios 1.A for both LD and HD districts. The use of the RES simulator produces the results summarized in Table 6.

The energy production potential of the system (brine-limited wastewater) is equal to 33421.58 kWh/year and 8058.44 kWh/year, respectively for the two cases. These values are calculated considering a functioning time of about 8000 hours per year (taking into account stops for maintenance and faults). The values, when referred to the energy purchased in the two districts, lead to the conclusion that a coverage of 10.20% and 10.86% of the energy purchased from the grid can be obtained by the RED system in the HD and LD districts, respectively. These values are obtained extracting the percentage from the *Grid Purchases* in Table 3. Instead, considering the overall load of the district reported in Table 2, the energy produced by the RED system covers the 6.63% and 6.76% of the overall energy need of the HD and LD districts, respectively, as shown in Figure 13. The diagrams in Figure 11 show that the SGP technology reduces the quantity of electric energy taken from the distribution grid, increasing the quota of renewable energy consumption of both the LD and HD district.

Table 5. Input data for Scenario 1.A.

	LD district	HD district
N° cell pairs, N	500	1500
Concentration, C		
HC	4.00 mol/l	4.00 mol/l
LC	0.01 mol/l	0.01 mol/l
Velocity, v		
HC	1.00 cm/s	1.00 cm/s
LC	0.16 cm/s	0.27 cm/s

Flow rate, Q		
HC	103.36 m³/day	310.07 m³/day
LC	16.54 m³/day	83.72 m³/day

Table 6. Report on produced power – Scenario 1A.

| Features	LD	HD
Gross power density, P_d	1.98 W/m² cell pair	2.77 W/m² cell pair
Corrected power density, $P_{d,corr}$	2.01 W/m² cell pair	2.79 W/m² cell pair
Gross power output, P	988.50 W $2.75 \cdot 10^{-4}$ kWh/s 1.43 kWh/m³ diluted 0.23 kWh/m³ concentrated	4152.32 W $1.15 \cdot 10^{-3}$ kWh/s 1.19 kWh/m³ diluted 0.32 kWh/m³ concentrated
Corrected power output, P_{corr}	1007.30 W $2.80 \cdot 10^{-4}$ kWh/s 1.46 kWh/m³ diluted 0.23 kWh/m³ concentrated	4177.70 W $1.16 \cdot 10^{-3}$ kWh/s 1.20 kWh/m³ diluted 0.32 kWh/m³ concentrated
Net gross power density	1.97 W/m² cell pair	2.77 W/m² cell pair
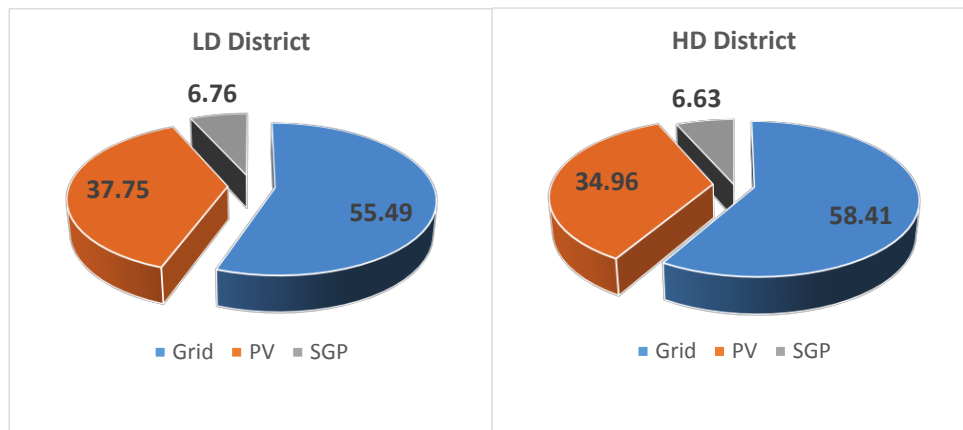
Fig. 13. Coverage of the total load of the district in Scenario 1.A.

In Scenario 1.B (representing the case of an urban center close to the sea and to a salt-works), the flow rate for the brine is limited by the RED system sizing. From the result of the REAPower project, the following quantity can be considered realistic: 300÷350 m³/day. The Input data for both districts are summarized in Table 7 while the results of the calculations are reported in Table 8.

Table 7. Input data for Scenario 1.B

	LD/HD districts
N° cell pairs, N	1500
Concentration, C	
HC	4.00 mol/l
LC	0.60 mol/l
Velocity, v	
HC	1.00 cm/s
LC	1.00 cm/s
Flow rate, Q	
HC	310.07 m^3/day
LC	310.07 m^3/day

Table 8. Report on produced power – Scenario 1.B.

Features	LD\HD
Gross power density, $\mathbf{P_d}$	2.33 W/m^2 cell pair
Corrected power density, $\mathbf{P_{d,corr}}$	2.34 W/m^2 cell pair
Gross power output, $\mathbf{P}$	3489.58 W
	9.69·10^{-4} kWh/s
	0.27 kWh/m^3 diluted
	0.27 kWh/m^3 concentrated
Corrected power output, $\mathbf{P_{corr}}$	3511.43 W
	9.75·10^{-4} kWh/s
	0.27 kWh/m^3 diluted
	0.27 kWh/m^3 concentrated
Net gross power density	2.32 W/m^2 cell pair

It can be observed that the production of the system brine-seawater is 28091.47 kWh/year. Also in this case the value is calculated considering a functioning time of about 8000 hours per year. When this result is referred to the energy purchased in the two districts, it leads to the conclusion that a coverage of respectively 8.57% and 37.85% of the energy purchased from the grid will be covered by the RED system in the HD and LD districts, respectively. Similarly, if referred to the overall load of the district, the energy produced by the

RED system will cover the 5.57% and 23.6% of the overall energy demand of the HD and LD district, respectively, as shown in Figure 14.

As shown in Figure 12, in the case of the LV district, thanks to SGP technology, the electricity from the grid is reduced to less than the 40% of the total need of the district.
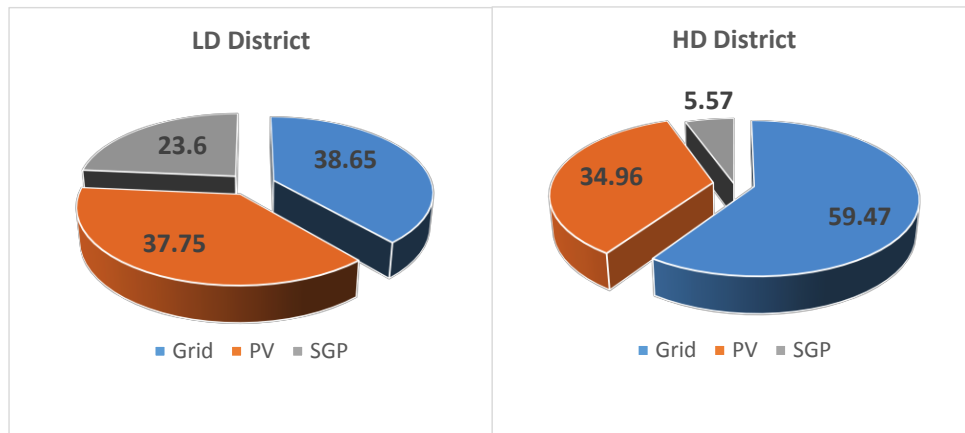

Fig. 14. Coverage of the total load of the district in Scenario 1.B.

Scenario 2

Scenario 2 represents the case of an urban center close to the sea but not to a salt-works. The effluents in this case are treated wastewater and seawater. This scenario considers a realistic case of limited wastewater production. The seawater concentration is assumed equal to $C_{HC,IN} = 0.6$ mol/l while the concentration of the wastewater as already considered is $C_{LC,IN} = 0.01$ mol/l. The input data for the simulations are reported in Table 9.

Table 9. Input data for Scenario 2.

	LD district	HD district
N° cell pairs, N	300	1000
Concentration, C		
HC	0.60 mol/l	0.60 mol/l
LC	0.01 mol/l	0.01 mol/l
Velocity, v		
HC	1.00 cm/s	1.00 cm/s
LC	0.26 cm/s	0.41 cm/s
Flow rate, Q		
HC	62.01 m³/day	206.71 m³/day
LC	16.12 m³/day	84.75 m³/day

As it can be easily understood, data are similar to those in Table 4 for case 1.A with the difference that the high concentration effluent shows a value $C_{HC,\ IN} = 0.6$ mol/l. The results of the RED simulator are reported in Table 10.

Table 10. Report on produced power – Scenario 2.

Features	LD	HD
Gross power density, $\mathbf{P_d}$	0.48 W/m^2 cell pair	0.73 W/m^2 cell pair
Corrected power density, $\mathbf{P_{d,corr}}$	0.49 W/m^2 cell pair	0.73 W/m^2 cell pair
Gross power output, $\mathbf{P}$	144.62 W	729.94 W
	4.02·10^{-5} kWh/s	2.03·10^{-4} kWh/s
	0.22 kWh/m^3 diluted	0.21 kWh/m^3 diluted
	0.06 kWh/m^3 concentrated	0.08 kWh/m^3 concentrated
Corrected power output, $\mathbf{P_{corr}}$	147.91 W	734.6 W
	4.11·10^{-5} kWh/s	2.04·10^{-4} kWh/s
	0.22 kWh/m^3 diluted	0.21 kWh/m^3 diluted
	0.06 kWh/m^3 concentrated	0.09 kWh/m^3 concentrated
Net gross power density	0.48 W/m^2 cell pair	0.73 W/m^2 cell pair

The quantity of seawater is considered unlimited, while wastewater has the same flow rate as case 1.A. The energy production of the system seawater-wastewater is 1183.31 kWh/year and 5876.79 kWh/year for LD and HD district, respectively. The electricity produced by the RED technology will cover 1.59% and 1.79 % of the electricity for LD district and HD district, respectively. Considering the overall electricity consumed by the districts, the RED technology will respectively cover 0.99% and 1.17% of the overall electricity need of the LD and HD districts, as shown in Figure 15.

The diagrams in Figure 3 show that, in scenario 2, the SGP technology is not able to provide a significant reduction of the energy exchange between the district and the main distribution grid.
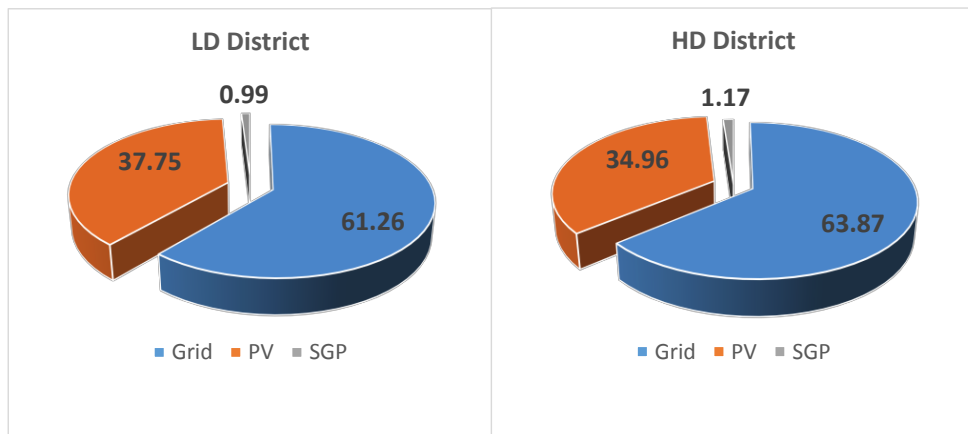
Fig. 15. Coverage of the total load of the district in Scenario 2.

5. Discussion

5.1. Influence of the urban features on the SGP system

It is interesting to analyze the relation between urban and energy features in order to understand what is the impact of the considered energy supply solution as the urban features change in the three examined cases 1.A, 1.B and 2. The analysis is done by defining the parameter Tdix, accounting for the urban density and defined as the ratio between the volume of the district's buildings and the surface area where they reside. Tdix assumes the following values for the two considered districts [48]:

$Tdix_{LD} = 0.73 \text{ m}^3/\text{m}^2$

$Tdix_{HD} = 2.06 \text{ m}^3/\text{m}^2$

As function of Tdix, Figures 14 to 16 show:

- the coverage by RED system of the electricity purchased from the grid (Figure 16);
- the RED system volume (Figure 17);
- the RED system power density (Figure 18).

Figure 16 shows that the coverage of the electricity purchased from the grid by the RED system has not an unique trend (increasing or decreasing) as the urban density varies, for the three scenarios considered in this study. The RED design indeed requires the choice of a number of cell pairs compatible with the flow rate of wastewater and a realistic salt concentration in the outgoing effluents. For each scenario and urban density, the overall maximum production potential was considered among the different explored configurations. Therefore, it is meaningful the result attained in the 1.A scenario for which up to 10.86% and 10.20% or the electricity purchased from the grid could be covered in the LD and HD districts, respectively. On the other

hand, scenario 2 shows a reduced production due to the reduced salinity concentration of seawater as compared to brine. This results in a very low coverage rate of the district's consumptions that, for both the LD and HD district, does not reach 2% of the total energy requested by the load. In scenario 2, therefore, the SGP system has a negligible effect on the energy balance of the two districts, as shown also in Figure 15.

Figure 17 shows the volume of the stack for all the considered cases, calculated as indicated in Table 11 assuming that, due to the spacers, a stack of 1000 cell pairs can occupy a volume of 1.5 m³. As it can be observed, volumes are perfectly adequate for building installations, since they vary between 0.45 and 2.25 m³. The larger stack volume is the one where effluents have unlimited flow rate (scenario 1.B). Considering an installation with parallel connected stacks, the overall volume occupation and corresponding outputted power can be increased and reaches 16.5 m^3. Technical rooms containing RED units do not need any particular conditioning, do not cause any risky situation for people and they neither produce noise. The specific power density is represented in Figure 18. Power density is expressed in kW/m³ and is a parameter that gives an indication of the effectiveness of the system. Figure 16 shows that the highest values of the power density parameter are for scenario 1.A, while scenario 2 appears the less efficient scenario.
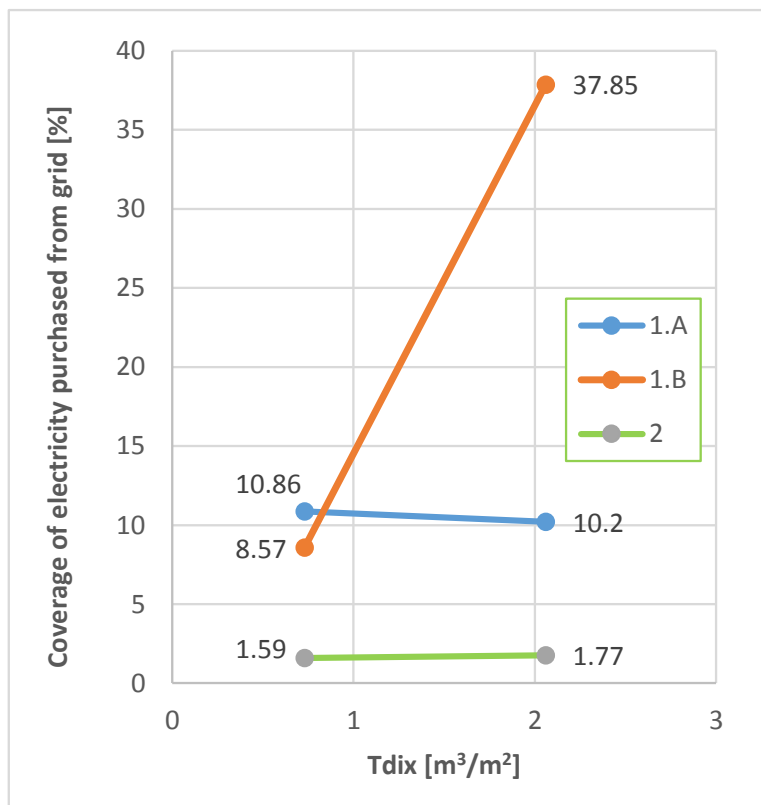

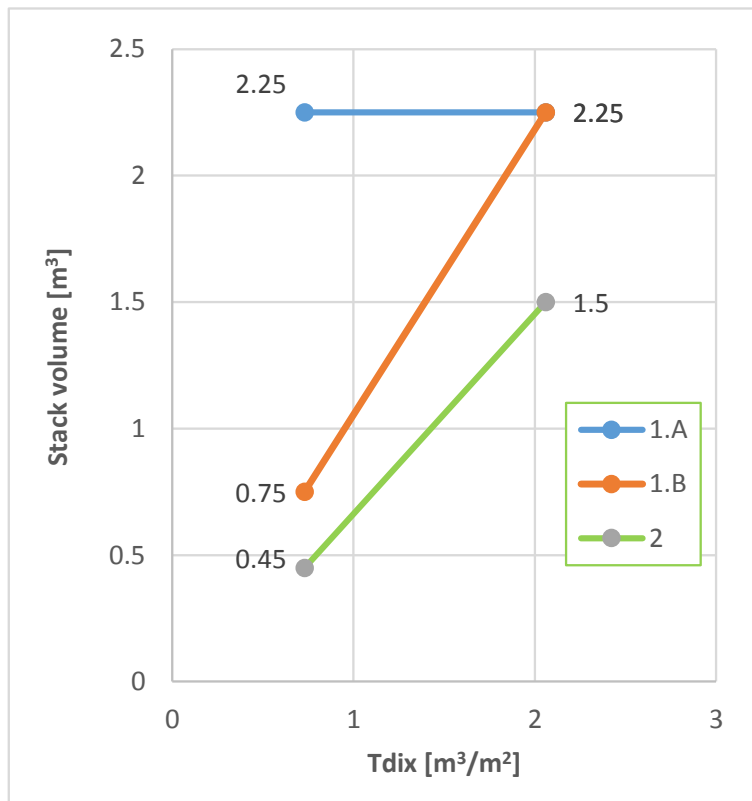*Fig. 16. Coverage of electricity purchased from grids.*
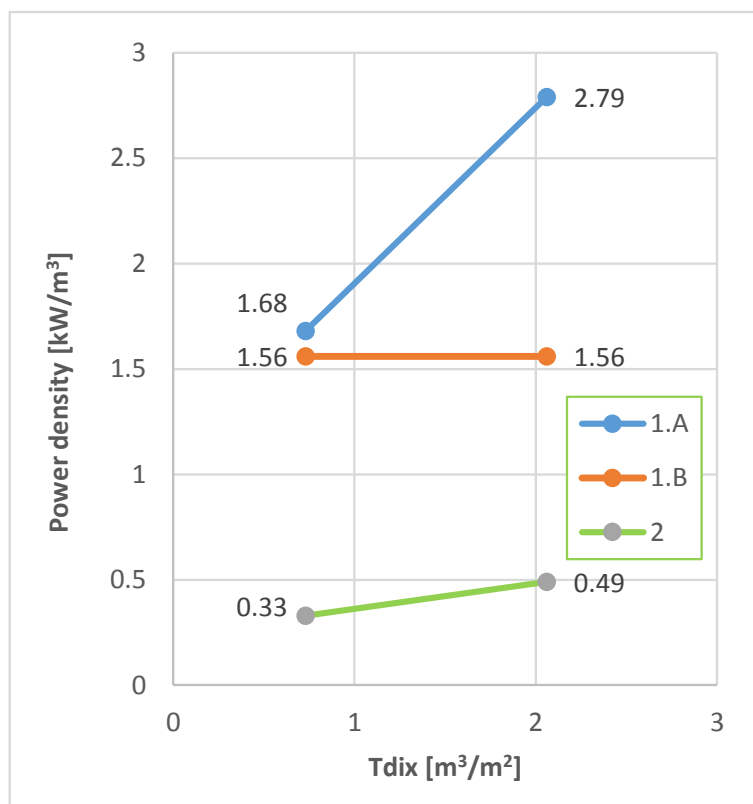
Fig.17. RED Stack volume.

Fig. 18. RED power density.

Table 11. RED Stack volume evaluation.

Scenario	LD	HD
1.A	From Table 5 there are 500 cell pairs $1000:1.5 \text{ m}^3 = 500:\text{V}$ $V=0.75 \text{ m}^3$	From Table 5 there are 1500 cell pairs $1000:1.5 \text{ m}^3 = 1500:\text{V}$ $V=2.25 \text{ m}^3$
1.B	From Table 7 there are 1500 cell pairs $1000:1.5 \text{ m}^3 = 1500:\text{V}$ $V=2.25 \text{ m}^3$	
2	From Table 9 there are 300 cell pairs $1000:1.5 \text{ m}^3 = 300:\text{V}$ $V=0.45 \text{ m}^3$	From Table 9 there are 1000 cell pairs $1000:1.5 \text{ m}^3 = 1000:\text{V}$ $V=1.5 \text{ m}^3$

5.2. Economic considerations

The feasibility study leads to the results summarized in Table 12.

Table 12. Installed power and energy production of the SGP system.

Scenario	LD	HD
1.A	Installed power: 0.9 kW Energy production: 8058.44 kWh/year	Installed power: 4.15 kW Yearly energy production: 33421.58 kWh/year
1.B	Installed power: 3.5 kW Energy production: 28091.47 kWh/year	
2	Installed power: 0.15 kW Energy production: 1183.31 kWh/year	Installed power: 0.74 kW Energy production: 5876.79 kWh/year

Since the RED technology is still at an experimental stage, it is not possible to provide a significant economic feasibility study of the proposed scenarios based on market prices. Nevertheless, it is realistic to suppose that in the next years, when SGP systems will be ready for commercialization, their initial cost will be still very high and their diffusion will need specific economic support mechanisms such as Feed-in tariffs, Green Tags or Tax credit, similarly to what happened in the past with PV, thermal solar and wind systems.

Concerning the economic feasibility of the proposed schemes, some recent information reported in the literature has indicated how it would be possible to reach a Levelised Cost of Electricity (LCOE) around 105 €/MWh [49]. Of course, such figure can only be seen as an indication for perspectives analysis of this novel technology, which has shown a good potential to become competitive with other RESs.

For evaluating the competitiveness of such systems with other kinds of distributed generators, it is interesting to compare the results obtained in the study with other feasible scenarios considering the installation of ground-mounted PV systems or micro-wind turbines.

This can be done starting from the yearly energy production values in Table 12 and evaluating the nominal power of a PV system and a wind turbine able to produce the same amount of energy in one year. Using the solar irradiation data of Mussomeli, the size of the PV system is calculated for all the scenarios and population density and is reported in Table 13. The same table reports also the installation costs of the PV systems considering an average specific cost for the Italian market in the range 1100-1800 €/kW. The SGP system is competitive with the PV technology if is able to guarantee the same installation costs in Table 13 and the same technical life.

Table 13. Nominal power and installation cost of ground-mounted PV systems in the various scenarios.

Scenario	LD	HD
1.A	Nominal power: 5.44 kW Installation cost of the PV system: 6.6 k€	Nominal power: 22.58 kW Installation cost of the PV system: 25 k€
1.B	Nominal power: 18.98 kW Installation cost of the PV system: 21 k€	
2	Nominal power: 18.98 kW Installation cost of the PV system: 1.2 k€	Nominal power: 3.97 kW Installation cost of the PV system: 4.8 k€

Similarly, considering a value of electricity production from wind equal to 1900 kWh/year per installed kW (realistic value for Mussomeli) and an average specific cost for the Italian market equal to 3000-4000 €/kW for vertical axis wind turbine, the nominal power values and installation costs reported in Table 14 are calculated. By comparing the results in Table 13 and 14, it is worth to notice that SGP technology will be more easily competitive with wind micro-turbine than with PV systems, considering the current prices of these two renewable based technologies. An advantage with respect to wind turbine is the total absence of noise that make SGP technologies more suitable for realizations in urban contexts.

Table 14. Nominal power and installation cost of vertical axis micro-wind turbines in the various scenarios.

Scenario	LD	HD
1.A	Nominal power: 4.47 kW Installation cost of the PV system: 15.6 k€	Nominal power: 18.56 kW Installation cost of the PV system: 55 k€
1.B	Nominal power: 15.60 kW Installation cost of the PV system: 47 k€	

2	Nominal power: 0.66 kW Installation cost of the PV system: 2.6 k€	Nominal power: 3.26 kW Installation cost of the PV system: 12.4 k€

6. Conclusions and further studies

In this paper, a methodology is presented and a feasibility study for the application of a SGP generator is carried out for two urban districts. The technology of the SGP is based on RED process that has recently drawn a lot of attention due to the potential applicability in contexts where safety of people and limited visual impact are of primary importance. The literature on the subject of renewable energy production in cities does not provide sufficient clues to consider the subject sufficiently discussed. The two considered urban districts in the feasibility study show different population density and they are considered in different geographic locations and close to the sea or to a salt-works. The results show that the most promising realistic scenarios are those including treated wastewater and brine (1.A) and unlimited seawater and brine (1.B).

Further studies will be addressed towards the analysis of higher density buildings close to the sea. The possibility to exploit indeed higher quantities of wastewater derives from the urban density. In further studies, also the idea of using SGP technology and in particular RED/ED processes to store electricity under the chemical form will be analyzed.

References

[1] C. O. Henriques, D. H. Coelho, N. L. Cassidy, Employment impact assessment of renewable energy targets for electricity generation by 2020—An IO LCA approach, Sustainable Cities and Society, 26 (2016), pp. 519-530

[2] M. R. Mozafar, M. H. Moradi, M. H. Amini, A simultaneous approach for optimal allocation of renewable energy sources and electric vehicle charging stations in smart grids based on improved GA-PSO algorithm, Sustainable Cities and Society, 32 (2017), pp. 627-637

[3] Y. Noorollahi, R. Itoi, H. Yousefi, M. Mohammadi, A. Farhadi, Modeling for diversifying electricity supply by maximizing renewable energy use in Ebino city southern Japan, Sustainable Cities and Society, 34 (2017), pp. 371-384

[4] S. Dawood, T. Crosbie, N. Dawood, R. Lord, Designing low carbon buildings: A framework to reduce energy consumption and embed the use of renewables, Sustainable Cities and Society, 34 (2031), pp. 63-71

[5] M. J. Khana, A. K. Yadavb, L. Mathewa, Techno economic feasibility analysis of different combinations of PV-WindDiesel-Battery hybrid system for telecommunication applications in different cities of Punjab, India, Renewable and Sustainable Energy Reviews ,76 (2017) pp. 577–607

[6] L. Liu, Z. Wang, The development and application practice of wind–solar energy hybrid generation systems in China, Renewable and Sustainable Energy Reviews, 13 (2009), pp. 1504–1512

[7] M. Chandel, G.D. Agrawal, S. Mathur, A. Mathur, Techno-economic analysis of solar photovoltaic power plant for garment zone of Jaipur city, Case Studies in Thermal Engineering, Volume 2, March 2014, pp. 1–7

[8] N.W. Alnaser, R. Flanagan, W.E. Alnaser Potential of making—over to sustainable buildings in the Kingdom of Bahrain, Energy and Buildings, 40 (2008), pp. 1304–1323

[9] X. Zhang, M. Li, Y. Ge, G. Li, Techno-economic feasibility analysis of solar photovoltaic power generation for buildings. Appl Therm Eng, 108 (2016), pp. 362–371

[10]   K. Steemers, Energy and the city: density, buildings and transport, Energy and Buildings, 35, issue 1 (2003) pp. 3-14

[11]   A. Kylili, A. Fokaides, European smart cities: The role of zero energy buildings, Sustainable Cities and Society, 15 (2015), pp. 86-95

[12]   S. Kosai, C. Tan, Quantitative analysis on a zero energy building performance from energy trilemma perspective, Sustainable Cities and Society, 32 (2017), pp. 130-141

[13]   M. Beccali, S. Ferrari, Energy-environmental and cost assessment of a set of strategies for retrofitting a public building toward nearly zero-energy building target, Sustainable Cities and Society, 32 (2017), pp. 226-234

[14]   M. Geidl, G. Koeppel, P. Favre-Perrod, B. Klockl, G. Andersson, K. Frohlic, The Energy Hub–A powerful concept for future energy systems, Third annual Carnegie Mellon Conference on the Electricity Industry, Pittsburgh, 2007.

[15]   A. Parisio, C. D. Vecchio, G. Velotto, Robust Optimization of operations in energy hub, 2011 50th IEEE Conference on Decision and Control and European Control Conference, 2011, pp. 4943-4948.

[16]   M. R. Almassalkhi, A. Towle, Enabling city-scale multi-energy optimal dispatch with energy hubs, in 2016 Power Systems Computation Conference (PSCC), 2016, pp. 1-7.

[17]   K. Orehounig, G. Mavromatidis, R. Evins, V. Dorer, J. Carmeliet, Towards an energy sustainable community: An energy system analysis for a village in Switzerland, Energy and Buildings, 84 (2014), pp. 277-286.

[18]   K. Orehounig, R. Evins, V. Dorer, J. Carmeliet, Assessment of Renewable Energy Integration for a Village Using the Energy Hub Concept, Energy Procedia, 57 (2014), pp. 940-949.

[19]   M. Batić, N. Tomašević, G. Beccuti, T. Demiray, S. Vraneš, Combined energy hub optimisation and demand side management for buildings, Energy and Buildings, 127 (2016), pp. 229-241.

[20]   M. Sepponen, I. Heimonen, Business concepts for districts' Energy hub systems with maximised share of renewable energy, Energy and Buildings, 124 (2016), pp. 273-280.

[21]   P. D. Lund, J. Mikkola, J. Ypyä, Smart energy system design for large clean power schemes in urban areas, Journal of Cleaner Production, 103 (2015), pp. 437-445.

[22]   M. C. Bozchalui, S. A. Hashmi, H. Hassen, C. A. Canizares, K. Bhattacharya, Optimal Operation of Residential Energy Hubs in Smart Grids, IEEE Transactions on Smart Grid, 3, issue 4 (2012), pp. 1755–1766.

[23]   X. Zhang, M. Shahidehpour, A. Alabdulwahab, A. Abusorrah, Optimal Expansion Planning of Energy Hub With Multiple Energy Infrastructures, IEEE Transactions on Smart Grid, 6, issue 5 (2015), pp. 2302–2311.

[24]   G. Beccuti, T. Demiray, M. Batic, N. Tomasevic, S. Vranes, Energy hub modelling and optimisation: an analytical case-study, 2015 IEEE Eindhoven PowerTech, 2015, pp. 1–6.."

[25]   J. Allegrini, K. Orehounig, G. Mavromatidis, F. Ruesch, V. Dorer, R. Evins, A review of modelling approaches and tools for the simulation of district-scale energy systems, Renewable and Sustainable Energy Reviews, 52 (2015), pp. 1391-1404.

[26]   H. J. Queisser, Multiple carrier generation in solar cells, Solar Energy Materials and Solar Cells, 94 (2010), pp. 1927-1930.

[27]   R. Niemi, J. Mikkola, P. D. Lund, Urban energy systems with smart multi-carrier energy networks and renewable energy generation, Renewable Energy, 48 (2012), pp. 524-536.

[28]   S. Pazouki, M.-R. Haghifam, Optimal planning and scheduling of energy hub in presence of wind, storage and demand response under uncertainty, International Journal of Electrical Power & Energy Systems, 80 (2016), pp. 219-239.

[29]   A. Najafi, H. Falaghi, J. Contreras, M. Ramezani, Medium-term energy hub management subject to electricity price and wind uncertainty, Applied Energy, 168 (2016), pp. 418-433.

[30]   S. Pazouki, M.-R. Haghifam, A. Moser, Uncertainty modeling in optimal operation of energy hub in presence of wind, storage and demand response, International Journal of Electrical Power & Energy Systems, 61 (2014), pp. 335-345.

[31]   P. C. D. G. Matthias Schulze, Multi-Period Optimization Of Cogeneration Systems: Considering Biomass Energy For District Heating, 2nd Power Systems Modeling Conference, 2009.

[32]   J. Radjenovic, M. Matosic, I. Mijatovic, M. Petrovic D. Barcelo, Membrane Bioreactor (MBR) as an Advanced Wastewater Treatment Technology, in the Handbook of Environmental

Chemistry: Emerging Contaminants from Inductrial and Municipal Waste, Vol. 5, Springer, Berlin (2008).

[33]   R.E. Pattle, Production of Electric Power by mixing Fresh and Salt Water in the Hydroelectric Pile, Nature 174 (1954).

[34]   A. T. Jones, W. Finley, "Recent development in salinity gradient power," in OCEANS 2003. Proceedings, 2003, pp. 2284-2287 Vol.4.

[35]   J. Veerman and D. A. Vermaas, "4 – Reverse electrodialysis: Fundamentals," in *Sustainable Energy from Salinity Gradients*, 2016, pp. 77–133.

[36]   A. Cipollina, G. Micale, A. Tamburini, M. Tedesco, L. Gurreri, J. Veerman, J. S. Grasman, "5 – Reverse electrodialysis: Applications," in *Sustainable Energy from Salinity Gradients*, 2016, pp. 135–180.

[37]   J. Veerman, M. Saakes, S. J. Metz, and G. J. Harmsen, "Reverse electrodialysis: Performance of a stack with 50 cells on the mixing of sea and river water," *J. Memb. Sci.*, vol. 327, no. 1–2, pp. 136–144, 2009.

[38]   M. Tedesco, A. Cipollina, A. Tamburini, I. D. L. Bogle, and G. Micale, "A simulation tool for analysis and design of reverse electrodialysis using concentrated brines," *Chem. Eng. Res. Des.*, vol. 93, no. January, pp. 441–456, 2015.

[39]   J. Veerman, M. Saakes, S. J. Metz, and G. J. Harmsen, "Reverse electrodialysis: A validated process model for design and optimization," *Chem. Eng. J.*, vol. 166, no. 1, pp. 256–268, 2011.

[40]   D. A. Vermaas, M. Saakes, and K. Nijmeijer, 'Doubled power density from salinity gradients at reduced intermembrane distance', *Environ. Sci. Technol.*, vol. 45, no. 16, pp. 7089–7095, 2011.

[41]   M. Tedesco E. Brauns, A. Cipollina, G. Micale, P. Modica, G. Russo, J. Helsen, 'Reverse electrodialysis with saline waters and concentrated brines: A laboratory investigation towards technology scale-up', *J. Memb. Sci.*, vol. 492, no. May, pp. 9–20, 2015.

[42]   A. Daniilidis, D. A. Vermaas, R. Herber, and K. Nijmeijer, 'Experimentally obtainable energy from mixing river water, seawater or brines with reverse electrodialysis', *Renew. Energy*, vol. 64, pp. 123–131, 2014.

[43]   M. Tedesco, A. Cipollina, A. Tamburini, and G. Micale, "Towards 1 kW power production in a reverse electrodialysis pilot plant with saline waters and concentrated brines," *J. Memb. Sci.*, vol. 522, no. September, pp. 226–236, 2017.

[44]   M. Tedesco, C. Scalici, D. Vaccari, A. Cipollina, A. Tamburini, G. Micale, Performance of the first reverse electrodialysis pilot plant for power production from saline waters and concentrated brines, Journal of Membrane Science, 500 (2016), pp. 33-45.

[45]   A. Tamburini, M. Tedesco A. Cipollina, G. Micale, M. Ciofalo, M. Papapetrou, W. Van Baak, A. Piacentino, 'Reverse electrodialysis heat engine for sustainable power production', *Appl. Energy*, vol. 206, no. August, pp. 1334–1353, 2017.

[46]   M. Bevacqua, A. Carubia, A. Cipollina, A. Tamburini, M. Tedesco, G. Micale, Performance of a RED system with ammonium hydrogen carbonate solutions, Desalin. Water Treat. 3994 (2016) pp. 1–12.

[47]   Italian Legislative Decree 152/06, Testo unico ambientale.

[48]   E. Riva Sanseverino, V. D. Genco, G. Scaccianoce, V. Vaccaro, R. Riva Sanseverino, G. Zizzo, M. L. Di Silvestre, D. Arnone and G. Paternò, Urban Energy Hubs and Microgrids: Smart

Energy Planning for Cities, in New Challenges in Optimizing Energy Grids, Edited by M. La Scala, ISTE Wiley, 2017.

[49]   M. Papapetrou, Environmental aspects and economics of salinity gradient power (SGP) processes. In: A.Cipollina, G. Micale, Sustainable Energy from Salinity Gradients, Elsevier Inc., 2016, pages 315-335 (Chapter 10).